Star-Shape Poly(acrylic acid)-Composed Glass-Ionomer Cements: Effects of MW and Arm Number on Mechanical Properties

Jun Zhao,[1] Yiming Weng,[1] Dong Xie[1,2]

[1]*Weldon School of Biomedical Engineering, Purdue University, West Lafayette, Indiana 47907*
[2]*Department of Biomedical Engineering, Purdue School of Engineering and Technology, Indiana University-Purdue University at Indianapolis, Indianapolis, Indiana 46202*

Received 17 May 2010; accepted 23 September 2010
DOI 10.1002/app.33451
Published online 10 December 2010 in Wiley Online Library (wileyonlinelibrary.com).

ABSTRACT: This study reports the synthesis and characterization of the star-shape poly(acrylic acid)s with different arm numbers and molecular weight (MW)s. The effects of arm number and initiator concentration on the atom-transfer radical polymerization reaction kinetics and solution viscosity were studied. The effects of MW and arm number on mechanical properties were evaluated. The results showed that both arm number and MW had significant impacts on the polymerization kinetics, solution viscosity, mechanical strengths, and wear-resistance. Decreasing arm number and increasing initiator concentration increased the reaction rate. Increasing arm number and initiator concentration decreased the solution viscosity. Decreasing arm number and increasing MW increased mechanical strengths and wear-resistance. Within the limitations of this study, the experimental cement was 28% in compressive strength, 48% in compressive modulus, 39% in diametral tensile strength, 60% in flexural strength, and 62% in Knoop hardness higher but 19% in fracture toughness lower than commercial Fuji II LC cement. The abrasion and attrition of the experimental cement were only 1.3% and 9.5% of Fuji II LC. © 2010 Wiley Periodicals, Inc. J Appl Polym Sci 120: 2390–2399, 2011

Key words: glass-ionomer cement; ATRP; mechanical properties; MW; arm number; star-shape poly(acrylic acid)

INTRODUCTION

Glass-ionomer cements (GICs) have been an attractive dental restorative for decades due to their numerous advantages including low cytotoxicity, good thermal compatibility with tooth, direct adhesion to tooth and base metals, minimized marginal microleakage and inhibition of secondary cavities.[1–5] However, their low mechanical strength and poor wear-resistance have restricted them for use only at certain low stress-bearing sites such as Class III and Class V cavities.[6,7]

Much effort has been made to improve the mechanical strengths of GICs and the focus has been mainly on improvement of polymer backbone or matrix.[7–16] Two main strategies have been applied. One is to incorporate hydrophobic pendent (meth)acrylate moieties onto the polyacid backbone in conventional GIC to make it become light- or redox-initiated resin-modified GIC[10–13,15] and the other is to directly increase molecular weight (MW) of the polyacid.[14–16] As a result, the former has shown significantly improved tensile and flexural strengths as well as handling properties.[10–13,15] The strategy of increasing MW of the polyacid by either introducing amino acid derivatives or *N*-vinylpyrrolidone has also shown enhanced mechanical strengths[14–16]; however, the working properties were somehow compromised because strong chain entanglements formed in these high MW linear polyacids resulted in an increased solution viscosity.[14,15] Recently, a novel light-curable 4-arm star-shape glass-ionomer system has been developed.[17,18] The polymer was synthesized via an advanced polymerization technique—atom-transfer radical polymerization (ATRP). The formed GIC system has no monomer in it. Because of this unique nature, the system has demonstrated substantially higher mechanical strengths as compared to Fuji II LC.[19] In addition, the system demonstrated much better biocompatibility than two commercially sound light-cured GICs, Fuji II LC and Vitremer.[18] The system also exhibited dramatically improved wear-resistance, which can compete with some of the commercial resin composites.[20] The main purpose of using star-shape polymer was to improve the mechanical strengths of the current GICs by altering the molecular architectures of the polymers. The strategy has been found valid.[17–20]

Correspondence to: D. Xie (dxie@iupui.edu).
Contract grant sponsor: NIH; contract grant numbers: DE018333, DE020614-01.

The objectives of this study were to synthesize and characterize the star-shape poly(acrylic acid)s with different arm numbers and MWs and to evaluate the effects of arm number, initiator concentration, and MW on the ATRP reaction kinetics as well as solution viscosity of the synthesized polymers and the mechanical properties of the formed cements.

EXPERIMENTAL

Materials

1,1,1-Tris-(hydroxymethyl)-propane, pentaerythritol, dipentaerythritol, 2-bromoisobutyryl bromide (BIBB), triethylamine (TEA), CuBr, *N*,*N*,*N*′,*N*′,*N*″-pentamethyldiethylenetriamine (PMDETA), *dl*-camphoroquinone (CQ), 2-(dimethylamino)ethyl methacrylate (DMAEMA), pyridine, *tert*-butyl acrylate (*t*-BA), glycidyl methacrylate (GM), hydrochloric acid (37%), diethyl ether, dioxane, *N*,*N*-dimethylformamide (DMF), ethyl acetate (EA), and tetrahydrofuran (THF) were used as received from VWR International Inc (Bristol, CT) without further purifications. Light-cured glass-ionomer cement Fuji II LC and Fuji II LC glass powders were used as received from GC America Inc (Alsip, IL).

Synthesis of the GM-tethered star-shape poly(acrylic acid)s

The GM-tethered 3-arm star-shape poly(acrylic acid) or poly(AA) was synthesized similarly as described in our previous publication.[17] Briefly, 1,1,1-tris (hydroxymethyl)-propane in THF was used to react with BIBB in the presence of TEA to form the 3-arm initiator. *t*-BA in dioxane was then polymerized with the 3-arm initiator in the presence of CuBr/PMDETA catalyst complex via ATRP at 120°C. The resultant 3-arm poly(*t*-BA) was hydrolyzed with hydrochloric acid and dialyzed against distilled water. The purified star-shape poly(AA) was obtained via freeze–drying, followed by tethering with GM in DMF in the presence of pyridine.[17,19] The GM-tethered star-shape poly(AA) was recovered by precipitation from diethyl ether, followed by drying in a vacuum oven at room temperature. The 4-arm and 6-arm star-shape poly(AA)s were synthesized in a similar way as described above except that pentaerythritol and dipentaerythritol were used as a core, respectively. The synthesis scheme for the 3-arm star-shape poly (AA) is shown in Figure 1. The 6-arm star-shape poly(AA) polymers with different initiator concentrations were also studied. A total of six polymers with different arm number (A, B, and C) and initiator concentration (C, D, and E) were synthesized, as shown in Table I.

Characterization

The chemical structures of the synthesized initiators and polymers were characterized by proton nuclear magnetic resonance (^{1}H-NMR) spectroscopy on a 500 MHz Bruker NMR spectrometer (Bruker Avance II, Bruker BioSpin Corp., Billerica, MA) using deuterated dimethyl sulfoxide and chloroform as solvents. The MWs and MW distributions of the synthesized poly(*t*-BA)s were measured in THF via a Waters GPC unit (Waters Corp., Milford, MA) with standard GPC techniques, using a polystyrene standard.

The viscosities of the liquids formulated with the GM-tethered star-shape poly(AA)s and distilled water were determined at 23°C using a programmable cone/plate viscometer (RVDV-II + CP, Brookfield Eng. Lab. Inc., Middleboro, MA).

The fracture surface of the selected specimen from the FS test was observed at a magnification of 1500× using a scanning electron microscope (Model JSM 5310, JOEL Ltd, Tokyo, Japan). The specimens were vacuum sputter-coated with gold-palladium (Au-Pd), and a vacuum was used to dehydrate the coated specimens before SEM analysis.

Sample preparation

The experimental cements were formulated with a two-component system (liquid and powder).[17] The liquid was formulated with the GM-tethered polymer, water [polymer/water (P/W) ratio = 70/30, by weight], 0.9% CQ (photo-initiator, by weight), and 1.8% DMAEMA (activator). Fuji II LC glass powder was used to formulate the cements with a powder/liquid ratio of 2.7. Fuji II LC was used as control and prepared per manufacturer's instruction at the P/L ratio = 3.2.

Specimens were fabricated at room temperature according to the published protocol.[17] Briefly, the specimens were prepared following the geometries below: (1) cylindrical (4 mm in diameter × 8 mm in length) for compressive strength (CS); (2) cylindrical (4 mm in diameter × 2 mm in thickness) for diametral tensile strength (DTS); (3) rectangular (3 mm in width × 3 mm in thickness × 25 mm in length) for flexural strength (FS); (4) rectangular (4 mm in width × 2 mm in thickness × 20 mm in length), fitted with a sharp blade for generating 2-mm-long notch, for fracture toughness (FT); (5) cylindrical (4 mm in diameter × 2 mm in thickness) for microhardness, where the smooth surface at the diametral side was generated by pressing the cement against a glass microscopic slide before setting; and (6) rectangular (4 mm in width × 2 mm in thickness × 10 mm in length) for wear tests. All the specimens were exposed to blue light (EXAKT 520 Blue Light

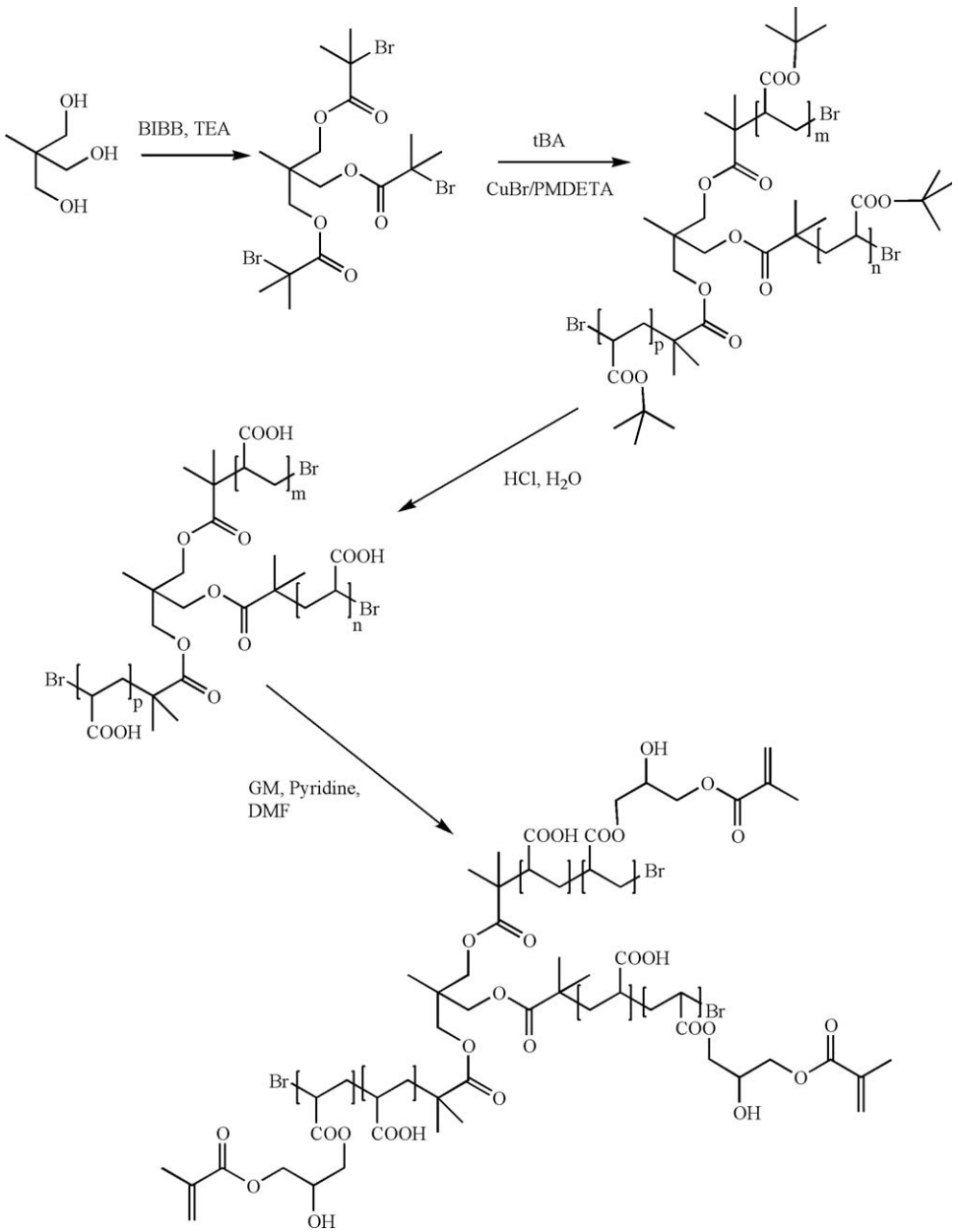

Figure 1 Reaction scheme for synthesis of the GM- tethered 3-arm star-shape poly(AA)

Polymerization Unit, GmbH, Germany) for 2 min, followed by conditioning in 100% humidity for 15 min and then in distilled water at 37°C for 1 week prior to testing.

Evaluation

CS, DTS, FS, and FT tests were performed on a screw-driven mechanical tester (QTest QT/10, MTS Systems Corp., Eden Prairie, MN), with a crosshead speed of 1 mm/min. The FS and FT tests were performed in three-point bending, with a span of 20 mm and 16 mm between supports, respectively. Six to eight specimens were tested to obtain a mean value for each material or formulation in each test. CS was calculated using an equation of $CS = P/\pi r^2$, where P = the load at fracture and r = the radius of the cylinder. DTS was determined from the relationship $DTS = 2P/\pi dt$, where P = the load at fracture, d = the diameter of the cylinder, and t = the thickness of the cylinder. FS was obtained using the expression $FS = 3Pl/2bd$,[2] where P = the load at fracture, l = the distance between the two supports, b = the breadth of the specimen, and d = the depth of the specimen. The FT was calculated from the equation $K_{IC} = \frac{P \cdot S}{B \cdot W} f(a/W)$, where K_{IC} = the index for FT, P = the load at fracture, S = the distance between supports, a = the length of notch, B = the

TABLE I
M_n, PDI, and Viscosity Values of the Synthesized Polymers

Code	Polymer	M_n (Dalton)[a]	PDI	Viscosity (cp)[b]
Effect of arm number				
A	3-arm (1%)	13,081	2.03	1505
B	4-arm (1%)	14,381	1.91	1157
C	6-arm (1%)	15,180	1.86	893
Effect of initiator concentration				
C	6-arm (1%)	15,180	1.86	893
D	6-arm (0.5%)	23,540	2.06	2654
E	6-arm (0.25%)	43,870	1.97	3808

[a] M_n and PDI of the synthesized poly(t-BA)s were determined by GPC.
[b] The viscosities of the GM-tethered poly(AA)s in water were measured at 23°C by a cone/plate viscometer; GM grafting ratio = 50%; P/W ratio = 60/40.

thickness of the specimen, and W = the width of the specimen. The f is a function of (a/W), as shown below[21]:

$$f(x) = \frac{3x^{0.5}[1.99 - x(1-x)(2.15 - 3.93x + 2.7x^2)]}{2(1+2x)(1-x)^{1.5}}$$

The hardness test was performed on a micro-hardness tester (LM-100, LECO Corp., MI) using a diamond indenter with 25 g load and 30 s dwell time. The Knoop hardness number (KHN) was averaged from six readings for each sample.

The wear test was conducted using the Oregon Health Science University (OHSU) oral wear simulator (Proto-tech, Portland, OR) using ceramic antagonists to produce both abrasive and attritional wear.[22,23] The test was performed following the procedures described by Turssi et al.,[24] with a slight modification. Briefly, after polishing with sand paper, the specimen embedded in the mold was tightened into an individual wear chamber, followed by the addition of a food like slurry consisting of 1.0 g ground poppy seed, 0.5 g poly(methyl methacrylate) powder, and 5 mL distilled water. The abrasion force was set at 20 N and the attrition force at 90 N. The specimen was subject to 70,000 wear cycles at a frequency of 1 Hz. The worn specimen was analyzed using an optical surface profilometer (Surftronic 3+, Taylor Hobson Ltd, Leicester, England).[24] Both abrasive and attritional wear depths were measured according to the manual for the profilometer, averaging from three traces. Four specimens were tested to obtain a mean wear value for each material or formulation.

Statistical analysis

One-way analysis of variance (ANOVA) with the *post hoc* Tukey-Kramer multiple-range test was used to determine significant differences of the measured properties among the materials in each group. A level of $\alpha = 0.05$ was used for statistical significance.

RESULTS AND DISCUSSION

Characterization

Figure 2 shows the ^{1}H-NMR spectra for BIBB and three synthesized star-shape initiators. The characteristic chemical shifts (ppm) are shown below: (a) BIBB: 2.00 (—$C(CH_3)_2$, 6 H); (b) 3-arm BIBB: 0.97 (—CCH_3, 3 H), 1.94 (—$C(CH_3)_2$, 18 H), and 4.19 (CCH_2O, 6 H); (c) 4-arm BIBB: 1.93 (—$C(CH_3)_2$, 24 H) and 4.32 (CCH_2O, 8 H); (d) 6-arm BIBB: 1.94 (—$C(CH_3)_2$, 24 H), 3.60 (—CCH_2OCH_2C—, 4 H), and 4.30 (—CCH_2O-, 12 H).

Figure 3 shows the ^{1}H-NMR spectra for *t*-BA, 6-arm BIBB, 6-arm poly(*t*-BA), 6-arm poly(AA), and GM-tethered 6-arm poly(AA). The characteristic chemical shifts are shown below: (a) *t*-BA: 1.50 (—CH_3, 9H), 5.68 (=CH_2, 1 H), 6.00 (=CHCO—, 1 H), and 6.27 (=CH_2, 1 H); (b) 6-arm BIBB: 1.94 (—$C(CH_3)_2$, 24 H), 3.60 (CCH_2OCH_2C, 4 H), and 4.30 (CCH_2O, 12 H); (c) 6-arm poly(*t*-BA): 1.44 (—CH_3), 1.83 (—CH_2—), and 2.22 (—CH—); (d) 6-arm poly(AA): 1.50 (—CH_3), 1.6–2.4 (—CH_2—), 3.0–3.7 (—CHCO—), and 12.48 (—COOH); (e) GM-tethered 6-arm poly(AA): 0.9–1.5 (—CH_3), 1.6–2.4 (—CH_2—), 1,88 (=CCH_3), 3.0–3.7 (—CHCO—), 3.8–4.2 (—OCH_2— on GM residues) 5.67 (CH_2=), 6.06 (CH_2=), and 12.25 (—COOH).

Polymerization kinetics

^{1}H-NMR was used to study the polymerization kinetics of *t*-BA during the ATRP reaction. To monitor the reaction, the aliquots retrieved from the reaction

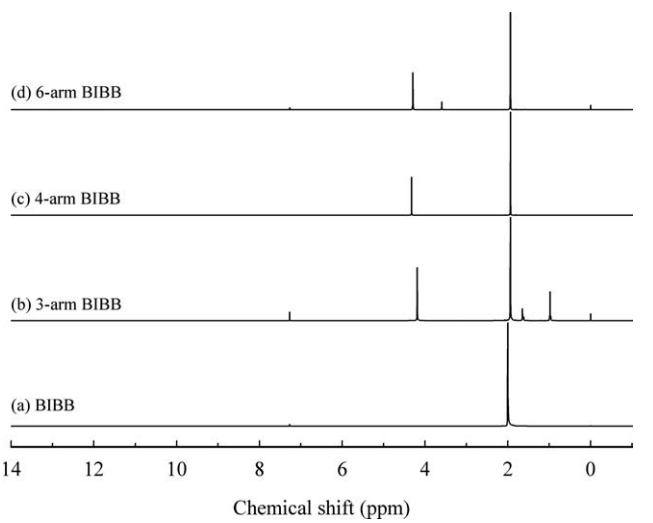

Figure 2 ^{1}H-NMR spectra: (a) BIBB, (b) 3-arm BIBB, (c) 4-arm BIBB, and (d) 6-arm BIBB

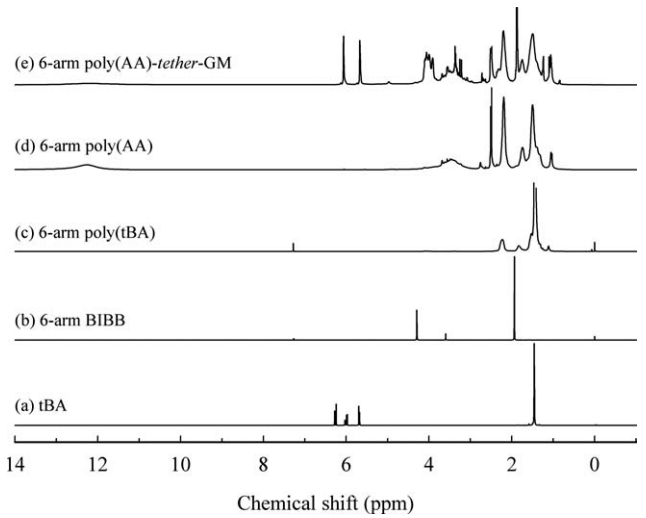

Figure 3 ^{1}H-NMR spectra: (a) *t*-BA, (b) 6-arm BIBB, (c) 6-arm poly(*t*-BA), (d) 6-arm poly(AA), and (e) 6-arm GM-tethered poly(AA)

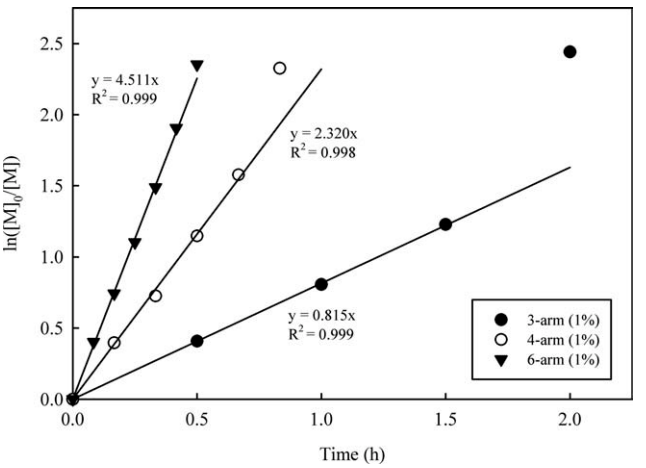

Figure 4 Kinetic plots of ln([M]$_0$/[M]) versus time for the polymerization of *t*-BA initiated with 3-, 4-, and 6-arm initiators: initiator/*t*-BA = 1% (by mole)

mixture at different time intervals were dissolved in $CDCl_3$ and analyzed with ^{1}H-NMR. The monomer concentration measured at each time point was converted to the conversion index ln([M]$_0$/[M]), which was then plotted against the reaction time, where [M]$_0$ = the initial monomer concentration and [M] = the monomer concentration at any time.

Figure 4 shows the effect of the arm number of the initiator on polymerization kinetics, where initiator = 1% (by mole) of *t*-BA and initiator/CuBr/PMDETA ratio = 1/0.25/0.75 (by mole). It was found that each plot remained linear until the ln([M]$_0$/[M]) value exceeded 2.0, where the monomer conversion = 86%. The slopes and R^2-values of the linear portions on the curves are 0.815 and 0.999, 2.320 and 0.998, and 4.511, 0.999 for the ATRP reactions of the 3-, 4-, and 6-arm initiators, respectively.

Figure 5 shows the effect of the 6-arm initiator concentration on polymerization kinetics, where initiator = 1%, 0.5%, and 0.25%. It was found that each plot remained linear until the ln([M]$_0$/[M]) value exceeded 1.6, where the monomer conversion = 80%. The slopes and R^2-values of the linear portions on the curves are 4.511 and 0.999, 1.285 and 0.998, and 0.355 and 0.997 for 1%, 0.5%, and 0.25%, respectively.

It is known that atom transfer radical polymerization (ATRP) can allow one to well control the polymerization rate of certain monomers and to make certain polymers to have special molecular architectures.[25] The polymerization rate of ATRP can be written as the equation: $-d[M]/dt = (k_p\ k_{act}/k_{deact})[M][R\text{-}X]_o[Cu\ (I)]/[Cu\ (II)\text{-}X] = k[M]$, where k_p = the polymerization rate constant, k_{act} = the rate constant of activating dormant species *R*-X into R$^\cdot$, k_{deact} = the rate constant of deactivating *R* into *R*-X, k = the apparent rate constant, and [M], [*R*-X]$_0$, [Cu (I)], and [Cu (II)-X] = the concentrations of monomer, initiating unit, Cu (I) and Cu (II)-X, respectively. Two assumptions were made when applying the general kinetics to this study: (1) the Cu (II) species had a very limited solubility when PMDETA was used as a ligand. This allowed Cu (II)-X to quickly reach the limiting value after the reaction started and thus [Cu (II)-X] could be viewed as constant during the reaction;[26] (2) [R-X]$_0$ and [Cu (I)] also remained constant for each reaction according to the amounts of the reagents added, although their values varied from reaction to reaction.[26] The ratio of CuBr/BIBB initiator unit was set to 1/4 for all the reactions shown in this study. Therefore, a first-order relation was obtained between ln([M]$_0$/[M]) and the reaction time t after integration, i.e., ln ([M]$_o$/[M]) = kt, where k = the apparent rate constant.

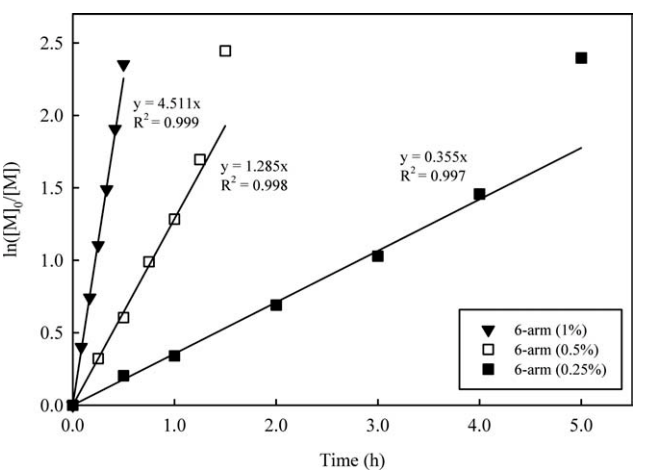

Figure 5 Kinetic plots of ln([M]$_0$/[M]) versus time for the polymerization of *t*-BA initiated with 6-arm initiator: initiator/*t*-BA (by mole) = 1%, 0.5%, and 0.25%

The plot of $\ln([M]_0/[M])$ versus time can be used to examine whether the reaction follows the pseudo-first order kinetics and to calculate the apparent rate constant k or the slop of the plot. As shown in Figures 4 and 5, all the plots exhibited a high linearity at the early stage of the polymerization (conversion = 80%). The R^2 values (0.997 to 0.999) indicate that the reactivity of the active sites remained constant during this stage. Once the monomer conversion reached 80%, the plot started to deviate from the linearity. This behavior may be explained below: (1) when the conversion was above 80%, the active sites moved to the ends of the long polymer chains, thus limiting their mobility; and (2) the viscosity of the reaction system became higher as the polymer grew. Both reasons led to reduction of the termination constant, resulting in an accelerated polymerization.[27,28] The plot deviation increased with increasing arm number or decreasing initiator concentration (or increasing MW) because more arms and higher MW aggravated the above two situations and thus accelerated the polymerization even significantly.

From Figure 4, the slop or k value of the plot for the polymerization was in the decreasing order: 6-arm initiator > 4-arm initiator > 3-arm initiator. This can be attributed to the reason that more arms indicate more initiating sites, thus leading to a faster ATRP reaction. From Figure 5, apparently the polymerization with a higher initiator concentration showed a higher k value, indicating that the higher the concentration of the initiator the faster the ATRP reaction.

MW and solution viscosity

Table I shows the number-average molecular weight (M_n) and polydispersity index (PDI) values of the synthesized poly(*t*-BA)s and viscosity values of the poly(AA)s in water. To avoid redundancy, the synthesized polymers were named as A = 3-arm (1%), B = 4-arm (1%), C = 6-arm (1%), D = 6-arm (0.5%), and E = 6-arm (0.25%), where 0.25%–1% represent the concentrations of the initiator. Apparently, the 3, 4, and 6-arm star-shape poly(*t*-BA)s with the same initiator/*t*-BA ratio showed a similar M_n. Decreasing the initiator concentration increased M_n. Increasing the arm number decreased the solution viscosity. C was 40% lower in viscosity than A although the former was 16% higher in M_n than the latter. With the same arm number, the polymer having a higher MW resulted in a higher solution viscosity. E was 2.9 times higher in MW and 4.3 times higher in viscosity than C.

The MW and solution viscosity of poly(alkenoic acid)s determine the mechanical strengths of GICs.[29] Poly(alkenoic acid) with high MW usually shows both high mechanical strength and viscosity.[29] The solution with high viscosity is hard to manipulate during the cement preparation, often resulting in voids and defects in the cement and thus reducing mechanical strength.[30] Generally both MW and solution viscosity need to be optimized to achieve high performance of GIC in mechanical strength. It is known that polymers with star-shape architectures have a lower intrinsic viscosity than linear polymers.[31] Therefore, optimizing the arm numbers and MWs of the star-shape poly(AA)s may help reduce the solution viscosity without compromising the mechanical strength.

The effects of arm number and initiator concentration on MW and viscosity of the star-shape poly(AA) were investigated, as shown in Table I. For the effect of the arm number, under the similar MW the 6-arm star-shape poly(AA) showed the lowest viscosity value but the 3-arm one showed the highest value. The more the arm number, the lower the viscosity. The 6-arm polymer that contained shorter polymer chains is much closer to a spherical structure than the 3- and 4-arm ones. The spherical molecular architecture can reduce the probability of intermolecular interactions and chain entanglements, thus leading to a lower solution viscosity.[31] On the other hand, having the same arm number (6-arm), the polymer with a higher MW showed a higher viscosity (see Table I). This can be attributed to the reason that the higher the MW the stronger the intermolecular interactions and chain entanglements.

Mechanical property evaluation

In this study, several common but very important tools were used to evaluate the mechanical properties of the experimental cements. These properties include CS, yield strength (YS), compressive modulus, DTS, FS, flexural modulus, flexural energy, FT, KHN, abrasion, and attrition. CS is important because many of the forces of mastication are compressive. DTS is necessary because most brittle materials like dental composite and cement are weak in tension and thus conventional tensile strength test is not suitable to GIC evaluation. FS is a collective measurement of three types of stress (tension, compression, and shear) simultaneously and measurement of FS offers the best practical and reliable estimate of tensile strength for brittle materials.[1] FT measures the ability of materials, especially relatively brittle materials, to resist crack initiation and propagation. FT is another important property in which GICs are often lower as compared to resin composites.[32] Wear-resistance is a measure of the ability of the material to resist mechanical wear. Abrasion and attrition are the most common wear phenomena encountered during the chewing cycle.[33,34] Abrasion is caused by frictional surface interactions

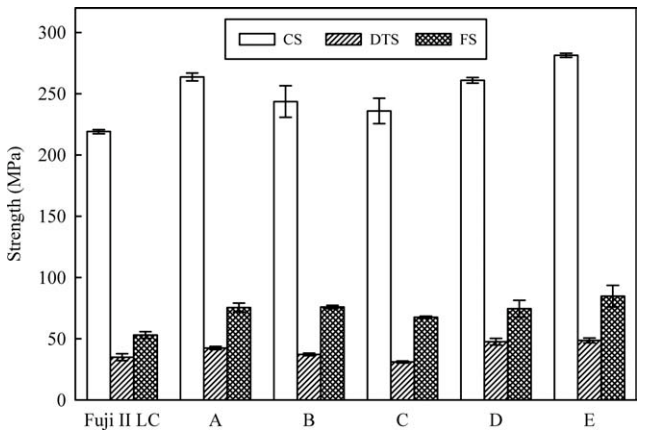

Figure 6 CS, DTS, and FS of the experimental cements: A = 3-arm (1%), B = 4-arm (1%), C = 6-arm (1%), D = 6-arm (0.5%), and E = 6-arm (0.25%). GM grafting ratio = 50% (by mole); P/W ratio = 70/30 (by weight); P/L ratio = 2.7/1 (by weight). Specimens were conditioned in distilled water at 37°C for 1 week prior to testing.

with toothbrush, toothpaste, food bolus, and fluid components during chewing. This type of wear is considered an important mechanism of occlusal material loss with resin composites. Attrition is caused by direct contact of sharp roughness asperities of the antagonist, which should at least be about 50% harder than the wearing substrate for substantial wear to occur. Attrition may cause substantial changes in surface texture (roughness, smear layer, etc).[34]

Figure 6 shows the CS (MPa), DTS (MPa), and FS (MPa) values of the experimental and Fuji II LC cements. For the effect of the arm number, CS: A > B > C > Fuji II LC, where B, C, and Fuji II LC were not significantly different from each other ($P > 0.05$); DTS: A > B > Fuji II LC > C, where B and Fuji II LC as well as Fuji II LC and C were not significantly different from each other ($P > 0.05$); FS: B > A > C > Fuji II LC, where A and B were not significantly different from each other ($P > 0.05$). For the effect of the MW, CS: E > D > C > Fuji II LC, where C and Fuji II LC were not significantly different from each other ($P > 0.05$); DTS: E > D > Fuji II LC > C, where D and E as well as Fuji II LC and C were not significantly different from each other ($P > 0.05$); FS: E > D > C > Fuji II LC, where all were significantly different from one another ($P < 0.05$).

Table II shows the yield CS (YS, MPa), compressive modulus (GPa), flexural modulus (GPa), and flexural energy (N/mm) values of the experimental and Fuji II LC cements. For the effect of the arm number, YS: A > B > C > Fuji II LC, where A and B as well as B and C were not significantly different from each other ($P > 0.05$); Compressive modulus: B > A > C > Fuji II LC, where A and B were not significantly different from each other ($P > 0.05$); Flexural modulus: A > B > C > Fuji II LC, where B and C were not significantly different from each other ($P > 0.05$); Flexural energy: A > B > C > Fuji II LC, where A, B, and C were not significantly different from each other ($P > 0.05$). For the effect of the MW, YS: E > D > C > Fuji II LC, where C and D as well as D and E were not significantly different from each other ($P > 0.05$); Compressive modulus: E > D > C > Fuji II LC, where C and D were not significantly different from each other ($P > 0.05$); Flexural modulus: E > D > C >Fuji II LC, where C and D as well as D and E were not significantly different from each other ($P > 0.05$); Flexural energy: E > D > C > Fuji II LC, where C, D, and E were not significantly different from each other ($P > 0.05$).

TABLE II
YCS, Compressive Modulus, Flexural Modulus, and Flexural Energy of the Experimental Cements[a]

Code	Polymer	YS (MPa)[b]	Compressive modulus (GPa)	Flexural modulus (GPa)	Flexural energy (N/mm)
Control					
	Fuji II LC	125.7 (7.1)[c]	5.40 (0.28)	6.90 (0.30)^{VI}	4.25 (0.50)^{IX}
Effect of arm number					
A	3-arm (1%)	203.0 (6.9)^{I,II}	7.94 (0.11)^{IV}	8.52 (0.24)^{VII,VIII}	8.20 (1.01)^{IX}
B	4-arm (1%)	196.7 (3.4)^{I,II,III}	8.09 (0.20)^{IV}	7.30 (0.56)^{VI}	6.10 (1.30)^{IX}
C	6-arm (1%)	172.1 (4.9)^{III}	7.47 (0.14)^{V}	7.28 (0.43)^{VI}	5.73 (1.24)^{IX}
Effect of initiator concentration					
C	6-arm (1%)	172.1 (4.9)^{III}	7.47 (0.14)^{V}	7.28 (0.43)^{VI}	5.73 (1.24)^{IX}
D	6-arm (0.5%)	180.5 (3.1)^{II,III}	7.50 (0.19)^{V}	7.68 (0.32)^{VI,VII}	7.18 (1.61)^{IX}
E	6-arm (0.25%)	200.4 (11.8)^{I,II}	7.98 (0.16)^{IV}	8.84 (0.21)^{VII,VIII}	8.30 (0.97)^{IX}

[a] GM grafting ratio = 50%; P/W ratio = 70/30, P/L ratio = 2.7/1.
[b] YS = compressive stress at yield. Specimens were conditioned in distilled water at 37°C for 1 week prior to testing.
[c] Entries are mean values with standard deviations in parentheses and the mean values with the same roman numerals in each category were not significantly different ($P > 0.05$).

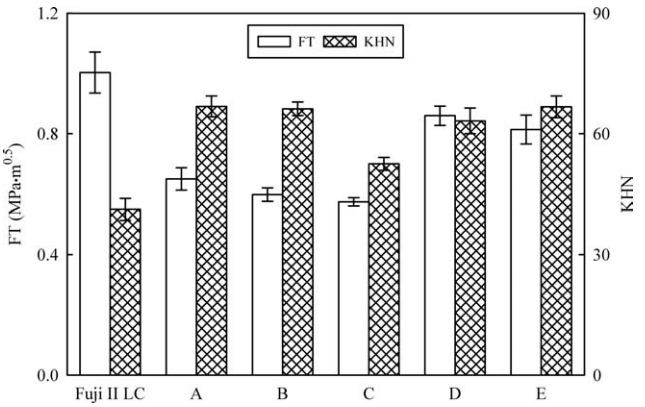

Figure 7 FT and KHN of the experimental cements: GM grafting ratio = 50%; P/W ratio = 70/30; P/L ratio = 2.7/1. Specimens were conditioned in distilled water at 37°C for 1 week prior to testing.

Figure 7 shows the FT (MPa/m$^{0.5}$) and KHN values of the experimental and Fuji II LC cements. For the effect of the arm number, FT: Fuji II LC > A > B > C, where A, B, and C were not significantly different from each other ($P > 0.05$); KHN: A > B > C > Fuji II LC, where A and B were not significantly different from each other ($P > 0.05$). For the effect of the MW, FT: Fuji II LC > D > E > C, where D and E were not significantly different from each other ($P > 0.05$); KHN: E > D > C > Fuji II LC, where D and E were not significantly different from each other ($P > 0.05$).

Figure 8 shows the abrasion and attrition values of the experimental and Fuji II LC cements. For the effect of the arm number, abrasion: Fuji II LC > A > B > C, where all were significantly different from one another ($P < 0.05$); attrition: Fuji II LC > A > B > C, where B and C were not significantly different from each other ($P > 0.05$). For the effect of the MW, abrasion: Fuji II LC > C > D > E, where all were significantly different from one another ($P < 0.05$); attrition: Fuji II LC > D > C > E, where all were significantly different from one another ($P < 0.05$).

Figure 9 shows the fracture surfaces of the optimal experimental cement and Fuji II LC from the FS test. It is apparent that the fracture surface with EXPGIC [Fig. 9(B)] looks rougher and more rugged than that with Fuji II LC [Fig. 9(A)]. The rugged and highly integrated fragments suggest that the experimental cement was a tougher material than Fuji II LC. In contrast, loosely bonded fragments are observed in Fuji II LC. On the other hand, more pores or voids are observed in EXPGIC [Fig. 9(B)], indicating more air bubbles trapped during the cement preparation.

From the results in Figures 6–8 and Table II, a general trend is observed, that is, the polymers with either fewer arms or higher MWs (or lower initiator concentration) showed higher mechanical strength values. As discussed above, under the similar MW fewer arms are equivalent to longer arms or longer polymer chains. On the contrary, more arms mean more star cores and shorter polymer chains. It should be emphasized that the star cores which are nothing but hydrocarbons in the polymers reduce the mechanical strengths because only carboxyl and methacrylate groups pendent on the polymer chains and intermolecular interactions as well as chain entanglements can make contributions to the strengths of the cement. The more the cores in the polymer, the lower the mechanical strengths of the formed cement. Therefore, longer arms or polymer chains which contain more carboxyl and methacrylate groups allow the cement to be higher in mechanical strengths through covalent and ionic crosslinks. That is why the cements with fewer arms showed higher mechanical strength values. It is known that MW is inversely proportional to initiator concentration. Therefore, a lower initiator concentration produces a polymer with a higher MW or a low initiator is equivalent to a high MW polymer. The higher values exhibited by the cements with higher MWs or lower initiator concentration (see Table II) are attributed to stronger intermolecular interactions and chain entanglements among the polymer chains. On the other hand, the polymers with fewer arms or higher MWs exhibited higher viscosity values than those with more arms or lower MWs (see Table I). Although there was no significant impact of viscosity on most of the measured mechanical strengths, the increased pores or voids on the fracture surface of the specimens with the experimental cement are obviously observed from the SEM photomicrographs (see Fig. 9). A difficulty in preparation of the cement E with the highest MW was also experienced during this study (see Table I). The result for K_{IC} values between the cement E and D may be another example

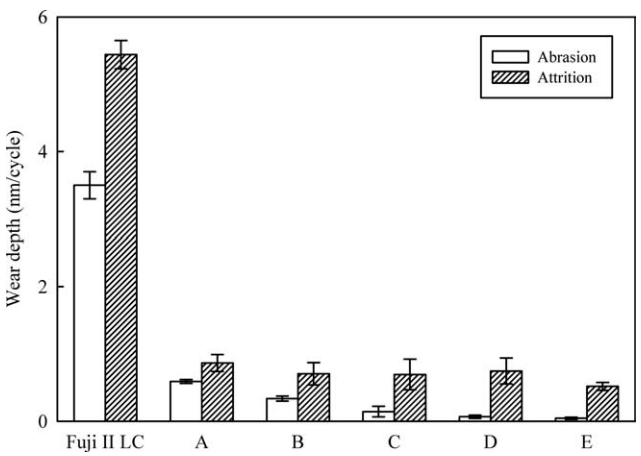

Figure 8 Abrasion and attrition in depth (nm/cycle) of the experimental cements: GM grafting ratio = 50%; P/W ratio = 70/30; P/L ratio = 2.7/1. Specimens were conditioned in distilled water at 37°C for 1 week prior to testing.

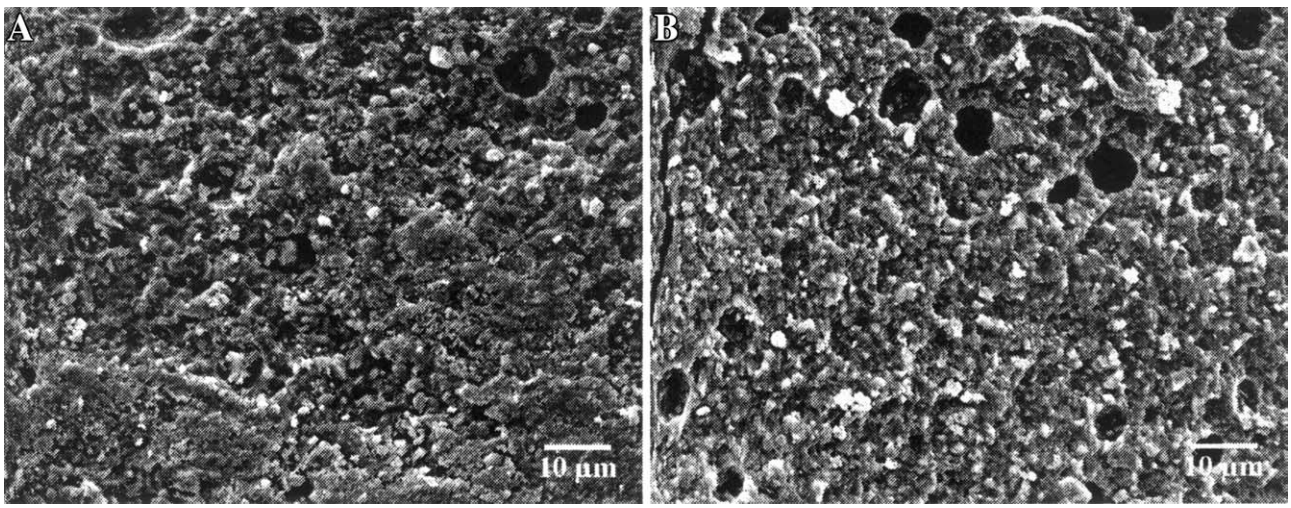

Figure 9 Fracture surface photomicrographs at a magnification of ×1500: (A) Fuji II LC; (B) EXPGIC: 6-arm (0.25%); GM grafting ratio = 50%; P/W ratio = 70/30; P/L ratio = 2.7/1. Specimens were conditioned in distilled water at 37°C for 1 week prior to testing.

to show the negative effect of the viscosity (Table I), where the former had a K_{IC} value of 0.814 but the latter had 0.860 (Fig. 7).

For abrasion and attrition, the similar trend is found for the effect of the MW, i.e., the higher the MW, the higher the wear-resistance. For the effect of arm number, the same trend is observed in attrition but not in abrasion. The polymers with fewer arms showed lower wear-resistance in abrasion (see Fig. 8). A possible explanation is given below: since the 6-arm polymer contains shorter polymer chains and more star cores than either 3- or 4-arm polymer under the similar MW, lower intermolecular interactions and chain entanglements are expected in its matrix. When the top layer of the polymer chains in the 6-arm polymer-composed cement was ripped off the cement surface during the abrasion, it was less likely for the inner layers of the polymer molecules to be pulled out simultaneously by the abrasion due to weaker intermolecular interactions and chain entanglement between the chains. Thus in each wear cycle less material was worn off from cement C as compared to cement A or cement B.

Mechanical property comparison between the experimental cement and Fuji II LC

Finally, the mechanical properties of commercial Fuji II LC cement were measured and compared with those of the experimental cement (E was chosen as the optimal one for comparison). Table III shows all the measured mechanical properties of the optimal experimental cement (EXPGIC) versus Fuji II LC. It was found that EXPGIC was 28% in CS, 48% in compressive modulus, 39% in DTS, 60% in FS, and 62% in KHN higher but 19% in FT lower than Fuji II LC. The abrasion and attrition of EXPGIC were only 1.3% and 9.5% of Fuji II LC. Apparently EXPGIC showed significantly higher mechanical strengths including CS, YS, compressive modulus, DTS, FS, KHN, and wear-resistance (abrasion and attrition), except for FT. The higher mechanical strengths exhibited by EXPGIC can be attributed to the nature of this unique experimental cement system. As mentioned in the section of Materials and Methods, EXPGIC was composed of star-shape poly(AA) polymer, water and initiators. There were no any low MW comonomers in it. Essentially this is a monomer-free cement system. The polymer aqueous liquid contains highly concentrated GM-tethered star-shape poly(AA), which not only provides a large quantity of carboxyl groups for salt-bridge formation but also a substantial amount of carbon–carbon double bond (methacrylate) for

TABLE III
Comparison of the Measured Properties Between Fuji II LC and EXPGIC[a]

Properties	Fuji II LC	EXPGIC
CS [MPa]	219.1 (1.7)[b]	281.4 (1.7)
Compressive modulus [GPa]	5.40 (0.28)	7.98 (0.16)
DTS [MPa]	34.9 (2.8)	48.6 (1.9)
FS [MPa]	53.0 (2.8)	84.7 (8.9)
FT [MPa/m$^{0.5}$]	1.00 (0.07)	0.81 (0.05)
KHN	41.2 (2.7)	66.7 (2.7)
Abrasion [nm/cycle]	3.49 (0.20)	0.04 (0.01)
Attrition [nm/cycle]	5.44 (0.21)	0.52 (0.06)

[a] Polymer = GM-tethered 6-arm star-shape poly(AA); initiator/t-BA = 0.25%; GM grafting ratio = 50%; *P/W* ratio = 70/30; P/L ratio = 2.7/1. Specimens were conditioned in distilled water at 37°C for 1 week prior to testing.

[b] Entries are mean values with standard deviations in parentheses and the two mean values in each category were significantly different from each other ($P < 0.05$).

covalent crosslinks. In contrast, in addition to linear poly(AA) and water, Fuji II LC contains a substantial amount of HEMA (2-hydroxylethyl methacrylate, a low MW monomer) and other low MW methacrylate or dimethacrylate comonomers,[11] which led to a lower strength as compared to EXPGIC. The fracture surface photomicrographs from SEM (Fig. 9) strongly supported the mechanical strength differences between the two cements. The higher K_{IC} in FT test exhibited by Fuji II LC may be attributed to a higher content of resin components such as methacrylate or dimethacrylate comonomers. These hydrophobic components usually contribute more to fracture toughness enhancement.[35] As we know, resin composites contain hydrophobic BisGMA and TEGDMA oligomers. That may partially be the reason why resin composites often show higher FT values than glass-ionomer cements.[1]

CONCLUSIONS

This study reports the synthesis and characterization of the star-shape poly(acrylic acid)s with different arm numbers and MWs. It was found that decreasing arm number and increasing initiator concentration increased the reaction rate. Increasing arm number and initiator concentration decreased the solution viscosity. Decreasing arm number and increasing MW increased mechanical strengths and wear-resistance. Within the limitations of this study, the experimental cement appears to be a better GIC cement than Fuji II LC due to its much higher mechanical performances.

References

1. Craig, R. Dental Restorative Materials; Mosby-Year Book, Inc.: St. Louis, MO, 1997.
2. Hume, W. R.; Mount, G. J. J Dent Res 1988, 67, 915.
3. Wiegand, A.; Buchalla, W.; Attin, T. Dent Mater 2007, 23, 343.
4. Lacefield, W. R.; Reindl, M. C.; Retief, D. H. J Prosthet Dent 1985, 53, 194.
5. Nicholson, J. W.; Braybrook, J. H.; Wasson, E. A. J Biomater Sci Polym Ed 1991, 2, 277.
6. Scholtanus, J. D.; Huysmans, M.-C. D. N. J. M. J Dent 2007, 35, 156.
7. Smith, D. C. Biomaterials 1998, 19, 467.
8. Wilson, A. D. Int J Prosthodont 1990, 3, 425.
9. Guggenberger, R.; May, R.; Stefan, K. P. Biomaterials 1998, 19, 479.
10. Mitra, S. B. J Dent Res 1991, 70, 72.
11. Momoi, Y.; Hirosaki, K.; Kohno, A.; McCabe, J. F. Dent Mater J 1995, 14, 109.
12. Xie, D.; Culbertson, B. M.; Johnston, W. M. J M S Pure Appl Chem 1998, A35, 1631.
13. Xie, D.; Wu, W.; Puckett, A.; Farmer, B.; Mays, J. Eur Polym Mater 2004, 40, 343.
14. Kao, E. C.; Culbertson, B. M.; Xie, D. Dent Mater 1996, 12, 44.
15. Xie, D.; Chung, I.-D.; Wu, W.; Lemons, J.; Puckett, A.; Mays, J. Biomaterials 2004, 25, 1825.
16. Xie, D.; Culbertson, B. M.; Johnston, W. M. J M S Pure Appl Chem 1998, A35, 1615.
17. Xie, D.; Park, J. G.; Zhao, J. Dent Mater 2007, 23, 395.
18. Xie, D.; Yang, Y.; Zhao, J.; Park, J. G.; Zhang, J. T. Dent Mater 2007, 23, 994.
19. Xie, D.; Zhao, J.; Park, J. G. J Mater Sci Mater Med 2007, 18, 1907.
20. Zhao, J.; Weng, Y.; Xie, D. Dent Mater 2009, 25, 526.
21. Johnson, W. W.; Dhuru, V. B.; Brantley, W. A. Dent Mater 1993, 9, 95.
22. Dowling, A. H.; Fleming, G. J. P. J Dent 2007, 35, 309.
23. Condon, J. R.; Ferracane, J. L. Dent Mater 1996, 12, 218.
24. Turssi, C. P.; Ferracane, J. L.; Vogel, K. Biomaterials 2005, 26, 4932.
25. Matyjaszewski, K.; Xia, J. Chem Rev 2001, 101, 2921.
26. Xia, J.; Matyjaszewski, K. Macromolecules 1997, 30, 7697.
27. Shipp, D. A.; Matyjaszewski, K. Macromolecules 1999, 32, 2948.
28. Shipp, D. A.; Matyjaszewski, K. Macromolecules 2000, 33, 1553.
29. Wilson, A. D.; McLean, J. W. Glass-Ionomer Cements; Quintessence Publ Co.: Chicago, IL, 1988.
30. Wu, W.; Xie, D.; Puckett, A.; Mays, J. Eur Polym J 2003, 39, 959.
31. Kakimoto, J. M. Prog Polym Sci 2001, 26, 1233.
32. Lloyd, C. H.; Adamson, M. Dent Mater 1987, 3, 225.
33. Sulong, M. Z. A. M.; Aziz, R. A. J Prosthet Dent 1990, 63, 342.
34. Lambrechts, P.; Goovaerts, K.; Bharadwaj, D.; De Munck, J.; Bergmans, L.; Peumans, M.; Van Meerbeek, B. Wear 2006, 261, 980.
35. Mitchell, C. A.; Douglas, W. H.; Cheng, Y. S. Dent Mater 2006, 15, 7.